Paper:

Simultaneous Learning of Robot Impedance Parameters Using Neural Networks

Mutsuhiro Terauchi*, Yoshiyuki Tanaka**, Seishiro Sakaguchi**, Nan Bu***, and Toshio Tsuji**

*Faculty of Psychological Sciences, Hiroshima International University
555-36 Kurose-Gakuendai, Higashi-Hiroshima, Hiroshima 724-0695, Japan
**Graduate School of Engineering, Hiroshima University
1-4-1 Kagamiyama, Higashi-Hiroshima, Hiroshima 739-8527, Japan
E-mail: tsuji@bsys.hiroshima-u.ac.jp
***National Institute of Advanced Industrial Science and Technology
807-1 Shunku, Tosu, Saga 841-0052, Japan

Impedance control is one of the most effective control methods for interaction between a robotic manipulator and its environment. Robot impedance control regulates the response of the manipulator to contact and virtual impedance control regulates the manipulator's response before contact. Although these impedance parameters may be regulated using neural networks, conventional methods do not consider regulating robot impedance and virtual impedance simultaneously. This paper proposes a simultaneous learning method to regulate the impedance parameters using neural networks. The validity of the proposed method is demonstrated in computer simulations of tasks by a multi-joint robotic manipulator.

1. Introduction

Impedance control is effective control for contacted objects such manipulators conducting tasks softly with a contacted object [1, 2]. Impedance control controls the response to external force by appropriately adjusting the mechanical impedance parameters for a controlled object; i.e., stiffness, viscosity and inertia. Conventional impedance control, however, which is performed using interaction force by contact between a manipulator and object, cannot be applied to tasks that doe not involve environmental contacts. Tsuji et al. [5, 6] and Nakabo et al. [7] proposed control methods for noncontact tasks by setting virtual impedance between controlled and contacted objects. Virtual impedance control proposed by Tsuji et al. assumes a virtual sphere at the hand of a manipulator, where virtual force is applied to the hand by setting virtual impedance between the hand and the approaching object. Nakabo et al., on the other hand, proposed a visual impedance control, where virtual impedance is set

from visual information, and torque calculated from the impedance is applied to each robot joint.

These methods have difficulties in calculating appropriate impedance parameters due to the need to consider nonlinear characteristics included in the controlled or contacted object. Parameters have been adjusted appropriately for tasks through learning using neural networks (NN), which is superior in nonlinear approximation. Gomi and Kawamoto [8], for example, proposed feedback control with NN learning as a nonlinear compensator for impedance control, and Jung and Hsia [9] proposed compensation adaptive to controller output by integrating NNs with a past position as input parallel to the controller. Tsuji et al. proposed a method of manipulator control for contact tasks adjusting mechanical impedance parameters set to a manipulator (hand impedance parameters) appropriately by repeated NN learning [10–13] and applied these to virtual impedance control, realizing manipulator response to movement of the contacted object [14].

Control with conventional impedance learning, however, requires adjustment for hand or virtual impedance parameters. Hand impedance control does not involve the concept of virtual impedance, limiting its application to tasks that have contact with contacted objects. Virtual impedance control, however, involves hand impedance where effects of impedance control are not appropriate without appropriate parameter setting. Since hand impedance parameters cannot be set by learning, adjustment relies on trial and error, making it difficult to determine parameters suitable for intended tasks.

We propose simultaneously learning both hand and virtual impedance during an operation to solve problems in the two types of impedance control and to achieve effective operation. We determined equations for hand impedance control and virtual control (Section 2), adjustment of NN impedance parameters (Section 3), and simulation results and the feasibility of our proposal (Section 4).
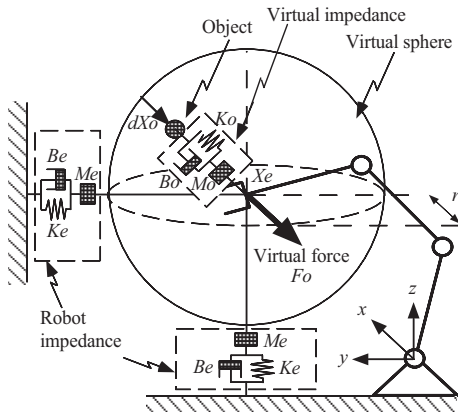
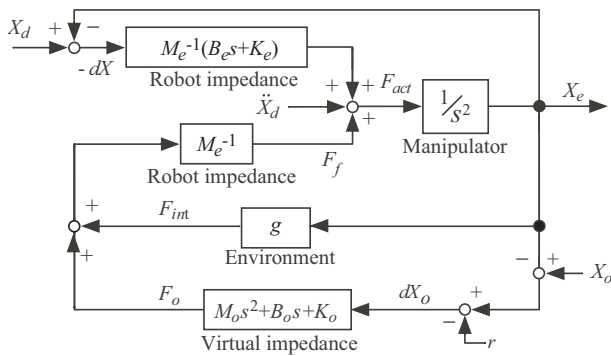**Fig. 1.** Schematic view of the proposed simultaneous impedance control.

Fig. 2. The block diagram of the simultaneous impedance control.

2. Impedance Control

Figure 1 shows our system concept and **Fig. 2** a control block diagram. Control involves hand impedance parameters to control responses to external force in contact with contacted objects and to control the manipulator trajectory in free movement, and virtual impedance parameters used for movement relative to the movement of contacted objects.

2.1. Hand Impedance Controller [12, 13]

When the degree of freedom (DOF) of the operating space is l, and that of a joint is m, the equation of motion for a manipulator in contacts with contacted objects is generally described as follows:

$$M(\boldsymbol{\theta})\ddot{\boldsymbol{\theta}} + h(\boldsymbol{\theta},\dot{\boldsymbol{\theta}}) = \tau + J^T(\boldsymbol{\theta})F_{int} \quad \ldots \quad (1)$$

where $\boldsymbol{\theta}, \dot{\boldsymbol{\theta}}, \ddot{\boldsymbol{\theta}} \in \Re^m$ represent the angle, angular velocity, and angular acceleration vector of a joint; $M(\boldsymbol{\theta}) \in \Re^{m \times m}$ an inertia matrix; $h(\boldsymbol{\theta},\dot{\boldsymbol{\theta}}) \in \Re^m$ a nonlinear term such as Coriolis force, joint friction, centrifugal force, or gravity; $\tau \in \Re^m$ a joint driving torque; $F_{int} \in \Re^l$ external force; and $J \in \Re^{l \times m}$ a Jacobian matrix.

Manipulator hand movement is dictated by:

$$M_e d\ddot{X} + B_e d\dot{X} + K_e dX = F_{int} \quad \ldots \ldots \quad (2)$$

where M_e, B_e, and $K_e \in \Re^{l \times l}$ represent a target inertia matrix, target viscosity matrix, and target stiffness matrix and $dX = X_e - X_d$ the deviation of current $X_e \in \Re^l$ from target hand position $X_d \in \Re^l$. Hand impedance (**Fig.2**) is set as $M_e^{-1}(B_e s + K_e)$ and M_e^{-1}.

2.2. Virtual Impedance Controller [14]

Assume that a virtual sphere of radius r with the center at the manipulator hand, and a contacted object is approaching the hand (**Fig. 1**). When the position of a contacted object is $X_o \in \Re^l$, normal vector dX_o from the surface of the virtual sphere to contacted object is described as follows:

$$dX_o = X_r - r\boldsymbol{n} \quad \ldots \ldots \ldots \ldots \quad (3)$$

where the vector from the hand to the contacted object is $X_r = X_o - X_e$, and vector $\boldsymbol{n} \in \Re^l$ is defined by:

$$\boldsymbol{n} = \begin{cases} \dfrac{X_r}{|X_r|} & (X_r \neq \boldsymbol{0}) \\ \boldsymbol{0} & (X_r = \boldsymbol{0}). \end{cases} \quad \ldots \ldots \ldots \quad (4)$$

When a contacted object enters the virtual sphere, virtual impedance is set between the contacted object and hand. Using virtual impedance and dX_o, virtual external force dX_o applied to the hand from the contacted object is defined as:

$$F_o = \begin{cases} M_o d\ddot{X}_o + B_o d\dot{X}_o + K_o dX_o & (|X_r| \leq r) \\ \boldsymbol{0} & (|X_r| > r) \end{cases} \quad (5)$$

where M_o, B_o, and $K_o \in \Re^{l \times l}$ represent a target inertia matrix, target viscosity matrix, and target stiffness matrix. As Eq. (5) indicates, when $|X_r| > r$, i.e., the contacted object is outside the virtual sphere, $F_o = \boldsymbol{0}$. Considering virtual impedance control, the equation of motion for the manipulator hand is described using Eqs. (2) and (5):

$$M_e d\ddot{X} + B_e d\dot{X} + K_e dX = F_{int} + F_o. \quad \ldots \quad (6)$$

External force F_o caused by virtual impedance M_o, B_o, K_o is applied before the contacted object touches the hand, and position and velocity control are conducted with hand impedance $M_e^{-1}(B_e s + K_e)$, generating hand movement. ($F_{int} = \boldsymbol{0}$). When $F_{int} \neq \boldsymbol{0}$, hand is restricted in contact with the contacted object, force is also controlled. In **Fig. 2**, virtual impedance is set as $M_o s^2 + B_o s + K_o$.

2.3. Impedance Control

Manipulator impedance control rules [2] for hand and virtual impedance are expressed as follows:

$$\tau = \tau_{effector} + \tau_{comp} \quad \ldots \ldots \ldots \quad (7)$$

$$\begin{aligned} \tau_{effector} = J^T \{ &M_x(\boldsymbol{\theta})[M_e^{-1}(-K_e dX - B_e d\dot{X}) \\ &+ \ddot{X}_d - \dot{J}\dot{\boldsymbol{\theta}}] - [I - M_x(\boldsymbol{\theta})M_e^{-1}]F_{int} \\ &+ M_x(\boldsymbol{\theta})M_e^{-1}F_o \} \quad \ldots \ldots \ldots \quad (8) \end{aligned}$$

$$\tau_{comp} = (\hat{M}^{-1}(\theta)J^T M_x(\theta)J)^T \hat{h}(\theta, \dot{\theta}) \quad . \quad . \quad . \quad (9)$$

$$M_x(\theta) = (J\hat{M}^{-1}(\theta)J^T)^{-1} \quad . \quad . \quad . \quad . \quad . \quad . \quad . \quad (10)$$

where $\hat{M}(\theta)$ represents an estimated inertia matrix, $\hat{h}(\theta, \dot{\theta})$ estimated $h(\theta, \dot{\theta})$, $\tau_{effector}$ joint torque for controlling the manipulator hand impedance, τ_{comp} joint torque for linear compensation for $h(\theta, \dot{\theta})$ in the equation of motion, and $M_x(\theta) \in \Re^{l \times l}$ is regular unless the arm is in an unusual position. Assuming that estimated $\hat{M}$ and $\hat{h}$ are close to true values, manipulator dynamics are linearized using designed control rules as follows:

$$\ddot{X}_e = F_{act} \quad . \quad . \quad . \quad . \quad . \quad . \quad . \quad . \quad . \quad . \quad . \quad . \quad (11)$$

where $F_{act} \in \Re^l$ represents control input expressed in the operating space.

Control input F_{act}, which realizes the above two types of impedance control, is as follows:

$$F_{act} = F_t + F_f + \ddot{X}_d \quad . \quad . \quad . \quad . \quad . \quad . \quad . \quad (12)$$

$$F_t = -M_e^{-1}(B_e d\dot{X} + K_e dX) \quad . \quad . \quad . \quad . \quad . \quad (13)$$

$$F_f = M_e^{-1}(F_{int} + F_o). \quad . \quad . \quad . \quad . \quad . \quad . \quad . \quad (14)$$

These enable a wide range of operations by adjusting impedance parameters by application. The next section will discuss the way to adjust these impedance parameters by learning with NN.

3. Simultaneous Robot Impedance Learning with NN

Formulated impedance parameters in the previous section are adjusted through repeated NN learning.

3.1. Online Learning

We realized smooth contact tasks by learning and controlling relative velocity and interaction between the manipulator and the environment before and after contact. Evaluation function $E(t)$ used in NN learning is defined as:

$$E(t) = E_f(t) + E_v(t) \quad . \quad . \quad . \quad . \quad . \quad . \quad . \quad (15)$$

where $E_f(t)$ is an evaluation function of external force applied to the manipulator hand, and $E_v(t)$ is that applied to velocity.

In hand impedance learning, M_e is involved in learning objects, and these three are controlled by adjusting M_e. Certain values are set for K_e and B_e [12, 13], and each NN is set for hand impedance M_e and virtual impedance K_o, B_o, and M_o, where NN weighting factors are renewed to minimize $E(t)$. In online learning, NN weighting factors are renewed to minimize $E_f(t)$ and $E_v(t)$ at predetermined sampling times. Impedance as NN output approaches a preferable value by modifying NN weighting factors w_{ij} to reduce $E_f(t)$ and $E_v(t)$ to the maximum.

Each modification amount Δw_{ij} for NN weighting factor w_{ij} is described as follows:

$$\Delta w_{ij} = -\eta \frac{\partial E(t)}{\partial w_{ij}} \quad . \quad . \quad . \quad . \quad . \quad . \quad . \quad . \quad (16)$$

$$\frac{\partial E(t)}{\partial w_{ij}} = \left(\frac{\partial E_f(t)}{\partial F_{act}(t)} + \frac{\partial E_v(t)}{\partial F_{act}(t)} \right) \frac{\partial F_{act}(t)}{\partial O(t)} \frac{\partial O(t)}{\partial w_{ij}}$$
$$. \quad . \quad . \quad . \quad . \quad . \quad . \quad (17)$$

where η represents a learning ratio, $F_{act}(t) \in \Re^l$ control input, and $O(t) \in \Re^{l \times 4}$ output of each NN. $\partial F_{act}(t)/\partial O(t)$ is calculated with Eqs. (11)-(14), and $\partial O(t)/\partial w_{ij}$ is calculated by the law of error propagation. $\partial E_f(t)/\partial F_{act}(t)$ and $\partial E_v(t)/\partial F_{act}(t)$, however, cannot be calculated directly due to manipulator dynamics.

$\partial E_f(t)/\partial F_{act}(t)$ and $\partial E_v(t)/\partial F_{act}(t)$ in Eq. (17) are approximated discretely to calculate the change in $E_f(t)$ or $E_v(t)$ to a minute change of $F_{act}(t)$, then modification is calculated for each NN weighting factor Δw_{ij} online. Learning for the hand and virtual impedance are detailed below.

3.2. Hand Impedance Learning

When the hand contacts a contacted object, external force F_{int} is applied to the hand by the contacted object. Since hand impedance M_e rolls to adjust the hand response to external force caused by contact, such evaluation is provided for M_e online learning involving F_{int} closer to the target value. The evaluation function for M_e adjustment is configured as follows:

$$E_f(t) = \frac{1}{2} \left(F_d(t) - F_{int}(t) \right)^2 \quad . \quad . \quad . \quad . \quad (18)$$

where $F_d(t)$ is a target interaction. Here, $\partial E_f(t)/\partial F_{act}(t)$ in Eq. (17) is developed into:

$$\frac{\partial E_f(t)}{\partial F_{act}(t)} = \frac{\partial E_f(t)}{\partial F_{int}(t)} \frac{\partial F_{int}(t)}{\partial F_{act}(t)}. \quad . \quad . \quad . \quad . \quad . \quad (19)$$

$\partial F_{int}(t)/\partial F_{act}(t)$ is further developed into:

$$\frac{\partial F_{int}(t)}{\partial F_{act}(t)} = \frac{\partial F_{int}(t)}{\partial X_e(t)} \frac{\partial X_e(t)}{\partial F_{act}(t)} + \frac{\partial F_{int}(t)}{\partial \dot{X}_e(t)} \frac{\partial \dot{X}_e(t)}{\partial F_{act}(t)}$$
$$+ \frac{\partial F_{int}(t)}{\partial \ddot{X}_e(t)} \frac{\partial \ddot{X}_e(t)}{\partial F_{act}(t)}. \quad . \quad . \quad . \quad . \quad (20)$$

For online M_e learning, stiffness, viscosity, and inertia of the contacted object must be measured accurately because learning is conducted by converting force control error to hand movement error. The model for the contacted object must be identified. For this, we used the method proposed by Tsuji et al. [12, 13], i.e., $\partial F_{int}(t)/\partial X_e(t)$, $\partial F_{int}(t)/\partial \dot{X}_e(t)$, and $\partial F_{int}(t)/\partial \ddot{X}_e(t)$ correspond to stiffness, viscosity, and inertia of the identified model of the contacted object. $\partial X_e(t)/\partial F_{act}(t)$, $\partial \dot{X}_e(t)/\partial F_{act}(t)$, and $\partial \ddot{X}_e(t)/\partial F_{act}(t)$ are approximated using the same with a sufficiently short sampling time.

3.3. Virtual Impedance Learning

Virtual impedance set between the manipulator hand and contacted object entering the virtual sphere must be
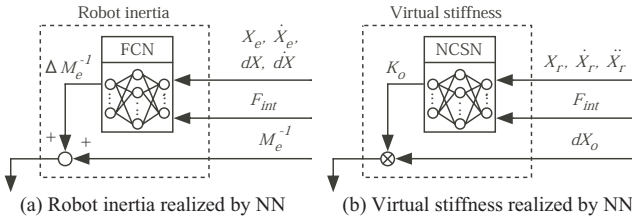
(a) Robot inertia realized by NN   (b) Virtual stiffness realized by NN

Fig. 3. Structure of FCN and NCSN.

Fig. 4. Components of robot impedance and virtual impedance.

adjusted based on the movement of the contacted object. Evaluation function $E_v(t)$ used for $\boldsymbol{K}_o$, $\boldsymbol{B}_o$, and $\boldsymbol{M}_o$ learning, is constituted with valuables relating to the movement of the hand and contacted object, i.e., position, velocity, and acceleration. An evaluation function, for example, to bring hand velocity closer to that of the contacted object is configured using two velocities:

$$E_v(t) = \frac{1}{2}\Big(\alpha(|\boldsymbol{X}_r|)\dot{\boldsymbol{X}}_o(t) - \dot{\boldsymbol{X}}_e(t)\Big)^2 \quad . . . \text{ (21)}$$

where $\alpha(|\boldsymbol{X}_r|)$ represents a gain function for smooth velocity change of the contacted object, set appropriately based on targeted tasks. $\partial E_v(t)/\partial \boldsymbol{F}_{act}(t)$ in Eq. (17) is developed using Eq. (21):

$$\frac{\partial E_v(t)}{\partial \boldsymbol{F}_{act}(t)} = \frac{\partial E_v(t)}{\partial \boldsymbol{X}_e(t)}\frac{\partial \boldsymbol{X}_e(t)}{\partial \boldsymbol{F}_{act}(t)} + \frac{\partial E_v(t)}{\partial \dot{\boldsymbol{X}}_e(t)}\frac{\partial \dot{\boldsymbol{X}}_e(t)}{\partial \boldsymbol{F}_{act}(t)}$$
$$+ \frac{\partial E_v(t)}{\partial \ddot{\boldsymbol{X}}_e(t)}\frac{\partial \ddot{\boldsymbol{X}}_e(t)}{\partial \boldsymbol{F}_{act}(t)}. \quad . . . . . . \text{ (22)}$$

$\partial \boldsymbol{X}_e(t)/\partial \boldsymbol{F}_{act}(t)$, $\partial \dot{\boldsymbol{X}}_e(t)/\partial \boldsymbol{F}_{act}(t)$, and $\partial \ddot{\boldsymbol{X}}_e(t)/\partial \boldsymbol{F}_{act}(t)$ are also approximated as in Section 3.2, enabling online learning for virtual impedance.

3.4. NN Configuration

Impedance is learned by NNs using the learning rules above. We set the Force Control Network (FCN) to learn $\boldsymbol{M}_e^{-1}$. FCN is a multilayer NN with input of hand position $\boldsymbol{X}_e$, hand velocity $\dot{\boldsymbol{X}}_e$, deviation $\boldsymbol{dX}$ between hand position $\boldsymbol{X}_e$ and target hand position $\boldsymbol{X}_d$, and deviation $\boldsymbol{dX}$ between hand velocity $\dot{\boldsymbol{X}}_e$ and target hand velocity $\dot{\boldsymbol{X}}_d$, and interaction $\boldsymbol{F}_{int}$, with the output of modification value $\Delta\boldsymbol{M}_e^{-1}$ of $\boldsymbol{M}_e^{-1}$. **Fig. 3(a)** shows the FCN. Note that FCN output is modified $\Delta\boldsymbol{M}_e^{-1}$, not $\boldsymbol{M}_e^{-1}$, because $\boldsymbol{M}_e^{-1}$ with a certain value is necessary for controlling the manipulator even when it is in free motion, and that $\boldsymbol{M}_e^{-1}$ is to be modified to a appropriate value for controlling external force applied to the hand upon contact with the contacted object.

Learning of virtual impedance in **Fig. 2** consists of three NNs, i.e., a noncontact stiffness network (NCSN), noncontact viscosity network (NCVN), and noncontact inertia network (NCIN). These NNs have input of relative position $\boldsymbol{X}_r$, relative velocity $\dot{\boldsymbol{X}}_r$, and relative acceleration $\ddot{\boldsymbol{X}}_r$ between the hand and contacted object, and interaction $\boldsymbol{F}_{int}$. The learning control configuration in **Fig. 2** is detailed in **Fig. 4**, and NCSN that output $\boldsymbol{K}_o$ is shown in **Fig. 3(b)**. NCVN and NCIN have configurations similar to that of NCSN.
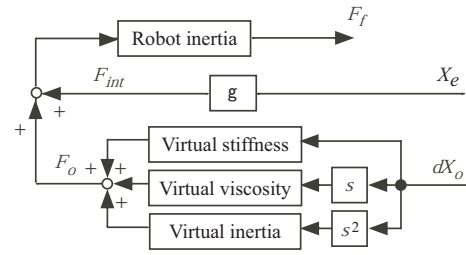
Each NN uses linear output functions in the input layer, and sigmoid functions in the middle and output layers. When each unit number is $i = \{1, 2, \ldots\}$ and $j = \{1, 2, \ldots\}$ (where $j < i$), and the input and output of units are x_i and y_i, they become:

$$x_i = \begin{cases} I_i & \text{(input layer)} \\ \sum w_{ij}y_j & \text{(middle and output layers)} \end{cases} . \text{ (23)}$$

$$y_i = \begin{cases} x_i & \text{(input layer)} \\ \dfrac{1}{1+e^{-x_i}} & \text{(middle layer)} \\ \dfrac{U}{2}\Big(\dfrac{1-e^{-x_i+\theta}}{1+e^{-x_i+\theta}}\Big) & \text{(output layer)} \end{cases} . . \text{ (24)}$$

where I_i represents an input of NN, w_{ij} a weighting factor from unit j to unit I, and $U \geq 0$ and $\theta \geq 0$ a maximum value and threshold of network output.

4. Experiment Results

Simulation results confirmed the feasibility of manipulator operation with the above two impedance parameters in online learning.

For simulation, each length of manipulator links was: $l = (l_1, l_2, l_3) = (0.30, 0.25, 0.27)$ [m], and the initial joint angle was $\theta = (\theta_1, \theta_2, \theta_3) = (\pi/2, \pi/9, 7\pi/18)$ [rad]. For initial manipulator hand impedance values: $\boldsymbol{K}_e = \text{diag}[500, 500, 500]$ [N/m], $\boldsymbol{B}_e = \text{diag}[250, 250, 250]$ [Ns/m], $\boldsymbol{M}_e = \text{diag}[10, 10, 10]$ [kg], and radius of the virtual sphere centered on the hand was $r = 0.2$ m. The sampling frequency was set to 1 kHz, considering a control experiment with a real machine.

4.1. Catching Task

The catching task involves receiving the contacted object approaching the manipulator hand from the outside without bouncing against it (**Fig. 5**). The contacted object is a ball at the end of a pendulum hung from the ceiling. To receive the contacted object, force applied to the hand or the contacted object upon contact must be small to contain the reaction, and the velocity of the hand must be close to that of the contacted object before contact to minimize relative velocity. We applied the evaluation function of Eq. (21) to NNs to adjust virtual impedance parameters
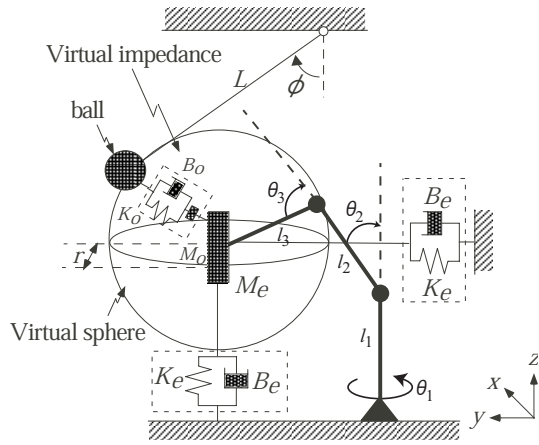
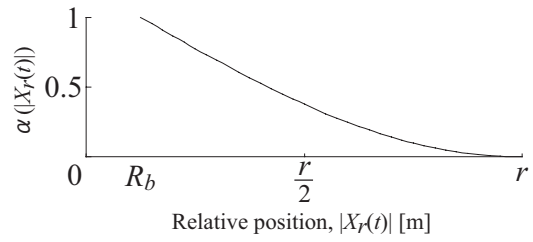**Fig. 5.** An experiment system of catching task.

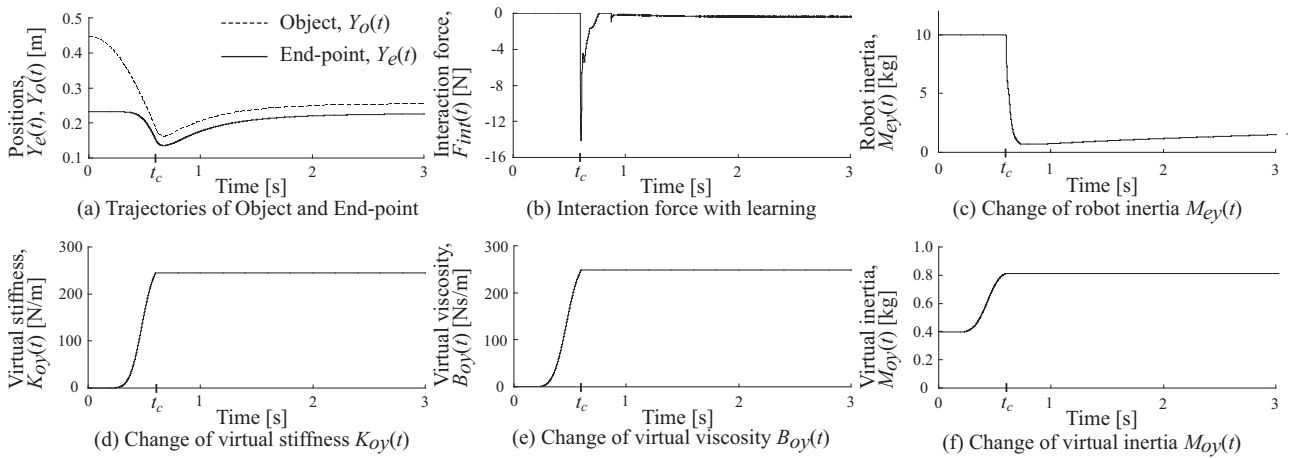**Fig. 6.** A gain function of catching task.

Fig. 7. Experimental results of the catching task.

for this task, and set gain function $\alpha(|X_r|)$ as follows:

$$\alpha(|X_r|) = \begin{cases} 1 - \sin\left(\dfrac{(|X_r| - R_b)\pi}{2(r - R_b)}\right) & (|X_r| \geq R_b) \\ 0 & (|X_r| < R_b) \end{cases} \quad (25)$$

where r and R_b represent radii of the virtual sphere and contacted object. The change of $\alpha(|X_r|)$ is shown in **Fig. 6**. For the evaluation function for learning hand impedance M_e, we used Eq. (18).

NNs used for learning have a 4-layer structure, each of which has 4 units in the input layer, 10 in the 2 middle layers, and 1 in the output layer. The initial weighting factors were provided with uniform random numbers $|w_{ij}| < 0.05$. The FCN learning ratio was $\eta_f = 0.0019$, NCSN learning ratio $\eta_p = 0.5$, NCVN learning ratio $\eta_v = 0.1$, and NCIN learning ratio $\eta_a = 0.0001$. The target interaction was set to $F_d = \text{diag}[0.0, -0.5, 0.0]$ [N], and the weight of the contacted object was $M_b = 0.5$ kg.

Figure 7(a) shows behaviors of hand and contacted object, **Fig. 7(b)** interaction by contact, **Fig. 7(c)** hand impedance M_e, and **Figs. 7(d)** to **(f)** time change (all toward the Y axis) of virtual impedance K_o, B_o, and M_o. K_{oy}, B_{oy}, and M_{oy} increased because it was necessary

to move the hand for approaching the contacted object (**Figs. 7(d)** to **(f)**). When the contacted object contacted the hand, M_{ey} decreased to reduce external force. In the figure, M_{ey} decreased once but gradually increased because interaction was less than a predetermined target when it became stationary after contact between the hand and contacted object, bringing the value closer to the target.

We confirmed with these results that both virtual impedance and hand impedance M_{ey} adjusted during operation. M_{ey} was learned by contact of the contacted object with the hand, and we studied the influence on learning when properties of the contacted object changed. **Fig. 8** shows changes in hand impedance M_{ey} in the direction of Y axis when weight M_b of the contacted object, was changed in catching tasks. The NN learning ratio for learning M_{ey} is fixed, so the greater the external force on the hand, the greater the change in M_{ey} to contain external force. As the weight of the contacted object increases, M_{ey} decreases (**Fig. 8**). External force generally increases with the weight of the contacted object. We confirmed that M_{ey} was learned based on the weight of the contacted object.
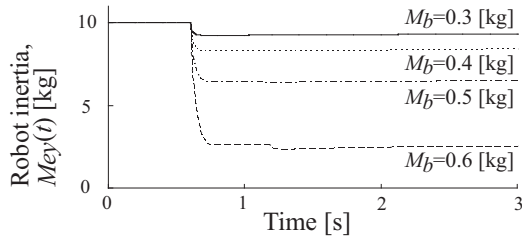
Fig. 8. Comparison of robot inertia.

Fig. 10. A gain function of tracing task.
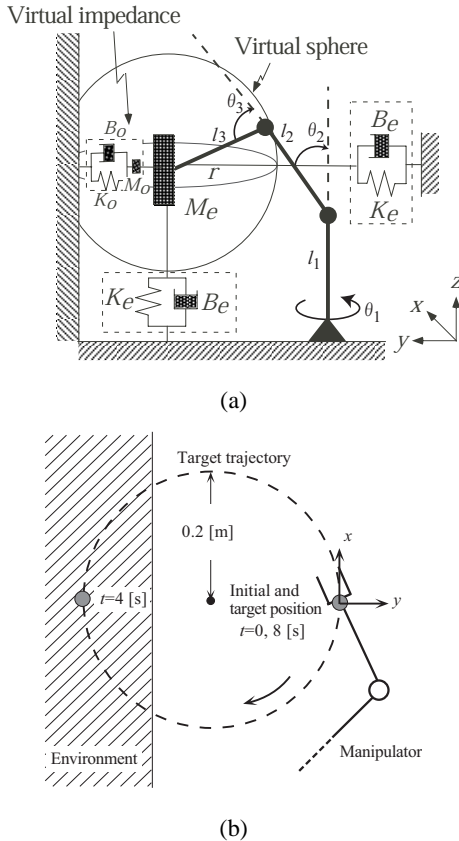

(a)

(b)

Fig. 9. An experiment system of tracing task.

4.2. Tracking Task

Catching tasks generate large external force on the hand for very short times. We verified performance with a tracking task in which a certain force is applied for a long time. Tracking is a task that, when there is a wall on the trajectory of the hand in free motion in space, traces the surface of the wall so that it does not apply excessive force upon contact (**Fig. 9**).

We studied a task in which the manipulator hand is programmed with a target trajectory to rotate counterclockwise for one turn for 8 s on a circle of 0.2 m in radius (**Fig. 9(b)**), and the manipulator traces the wall [12, 13]. Executing this task involves a strategy in which the velocity of the hand is reduced before contact, and external force on the hand is controlled to approach the target
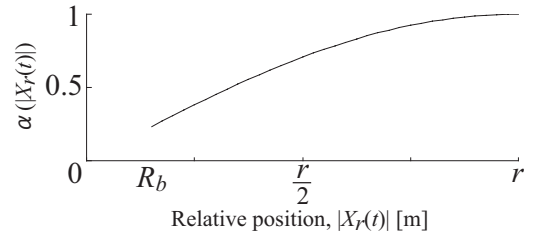
($F_d = 0$ N) after contact. We apply the same evaluation function for M_e learning, i.e., Eq. (18), used in the catching task, and the evaluation function to learn K_o, B_o, and M_o:

$$E_v(t) = \frac{1}{2}\left(\alpha(|X_r|)\dot{X}_e(t_c) - \dot{X}_e(t)\right)^2 \quad . \quad . \quad (26)$$

where $X_e(t_c)$ is the velocity of the hand at moment ($t = t_c$) when the virtual sphere entered the wall, and $\alpha(|X_r|)$ represents a gain function that smoothly changes the target velocity of the hand based on relative distance X_r between the hand and wall. The gain
function used in this study is:

$$\alpha(|X_r|) = \begin{cases} \sin\left(\dfrac{(|X_r|)\pi}{2r}\right) & (|X_r| \geq R_b) \\ 0 & (|X_r| < R_b). \end{cases} \quad (27)$$

Fig. 10 shows a change of $\alpha(|X_r|)$.

In simulation, wall viscoelasticity was set to: $K_c = \text{diag}[0, 10000]$ [N/m], $B_c = \text{diag}[0, 20]$ [Ns/m], and $M_c = \text{diag}[0, 0.1]$ [kg], and the target time trajectory of the hand given by a polynomial of degree 5 [15]. As in the catching task, 4-layer NNs were used for learning, and learning ratios were set to $\eta_f = 0.05$ for FCN, $\eta_p = 0.15$ for NCSN, $\eta_v = 0.1$ for NCVN, and $\eta_a = 0.0001$ for NCIN. The target interaction was set to $F_d = \text{diag}[0.0, 0.001, 0.0]$ [N].

Figure 11(a) shows position changes of the hand during tracking, **Fig. 11(b)** shows interactions with and without learning in comparison, **Fig. 11(c)** shows hand impedance M_e, and **Figs. 11(d)** to **(f)** show time changes in virtual impedance K_o, B_o, and M_o (all in the direction of the Y axis). As shown in **Figs. 11(d)** to **(f)**, virtual impedance K_{oy}, B_{oy}, and M_{oy} started changing when the virtual sphere at the hand contacted with the wall, so virtual force F_{oy} was applied to the hand to reduce the velocity of the hand before contact. Virtual impedance started changing again from 6 s because learning was conducted to reduce the velocity of the hand when the hand, contacting the wall, started to leave it. When the hand returns, there is no need to contain hand velocity, so no virtual external force is applied even if parameters are learned. After contact, external force on hand is reduced by lowering hand impedance M_{ey}. Although we applied a constant sampling time interval to this simulation, the interval may be automatically adjusted to shorter upon detecting a rapid change in the interaction, which may make a tracking task smoother.

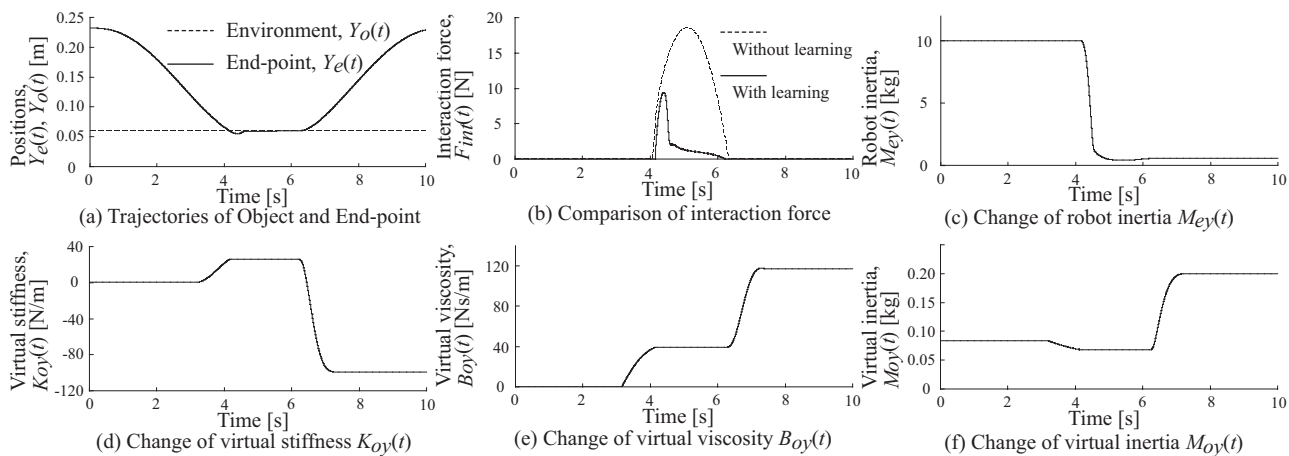As started, we achieved manipulator operation by con-

Fig. 11. Experimental results of the tracing task.

tacted objectives simultaneously adjusting hand and virtual impedance.

5. Conclusions

We have proposed simultaneously adjusting both hand and virtual impedance, studied little up to now. We demonstrated that impedance parameters are adjusted appropriately, enabling efficient operation taking advantages of both impedance controls. We will continue to study suitable NN configurations and setups for learning parameters, and will conduct verification with a real machine.

References:
[1] N. Hogan, "Impedance Control: An Approach to Manipulation, Parts I, II, III," ASME Journal of Dynamic Systems, Measurement, and Control, Vol.107, No.1, pp. 1-24, 1985.
[2] N. Hogan, "Stable Execution of contact tasks using impedance control," Proc. IEEE International Conference on Robotics and Automation, pp. 1047-1054, 1987.
[3] T. Sakaki and S. Tachi, "Contact Stability Analysis on Some Impedance Control Methods," Journal of the Robotics Society of Japan, Vol.12, No.3, pp. 155-162, 1994 (in Japanese).
[4] T. Sakaki and S. Tachi, "A Stabilizing Method of Contact Tasks on Servo-based Impedance Control," Journal of the Robotics Society of Japan, Vol.13, No.5, pp. 77-83, 1995 (in Japanese).
[5] T. Tsuji and M. Kaneko, "Non-Contact Impedance Control for Redundant Manipulators," IEEE Transactions on Systems, Man, and Cybernetics – Part A: Systems and Humans, Vol.29, No.2, pp. 184-193, March, 1999.
[6] T. Tsuji and M. Kaneko, "Non-contact Impedance Control for Redundant Manipulator," IEEE Transaction on Systems, Man, and Cybernetics – PartA, Vol.29, No.2, pp. 184-193, 1999.
[7] Y. Nakabo and M. Ishikawa, "Visual Impedance Using 1ms Visual Feedback System," In proceedings of the 1998 IEEE Int. Conf. Robotics and Automation, pp. 2333-2338, 1998.
[8] G. Gomi and M. Kawato, "Neural Network Control for a Closed Loop System Using Feedback-Error-Learning," Neural Networks, Vol.6, No.7, pp. 933-946, 1993.
[9] S. Jung and T. C. Hsia, "On Neural Network Application to Robust Impedance Control of Robot Manipulators," Proc. of IEEE Int. Conf. on Robotics and Automation, pp. 869-974, 1995.
[10] T. Tsuji, M. Nishida, and K. Ito, "Iterative Learning of Impedance Parameters for Manipulator Control Using Neural Networks," Transactions of the Society of Instrument and Control Engineers, Vol.28, No.12, pp. 1461-1468, 1992 (in Japanese).
[11] T. Tsuji, K. Ito, and P. Morasso, "Neural Network Learning of Robot Arm Impedance in Operational Space," IEEE Transaction on Systems, Man, and Cybernetics – PartB, Vol.26, No.2, pp. 290-298, 1996.
[12] T. Tsuji and Y. Tanaka, "On-line Learning of Robot Arm Impedance Using Neural Networks," Robotics and Autonomous Systems, Vol.52, No.4, pp. 257-271, 2005.
[13] T. Tsuji and Y. Tanaka, "On-line Learning of Robot Arm Impedance Using Neural Networks," Robotics and Autonomous Systems, Vol.52, No.4, pp. 257-271, 2005.
[14] T. Tsuji, M. Terauchi, and Y. Takana, "On-line Learning of Virtual Impedance Parameters in Non-contact Impedance Control Using Neural Networks," IEEE Transactions on Systems, Man, and Cybernetics – Part B: Cybernetics (Technical correspondence), pp. 2112-2118, 2004.
[15] T. Yoshikawa, "Foundations of Robot Control," Corona Publishing Co. LTD., 1988 (in Japanese).

Name:
Mutsuhiro Terauchi

Affiliation:
Faculty of Psychological Sciences, Hiroshima International University

Address:
555-36 Gakuendai, Kurose-cho, Kamo-gun, Hiroshima 724-0695, Japan
Brief Biographical History:
1989- Research Associate in Faculty of Engineering at Hiroshima University
1994- Research Associate in Faculty of Information Sciences at Hiroshima City University
1999- Visiting Scientist, University of California at Santa Cruz
2001- Lecturer of Department of Psychological Sciences at Hiroshima International University
Main Works:
• M. Terauchi and M. Nishikawa, "A Case Structure Based Translation System from Japanese Sentences with Analyzed Case Representation into Sign Language," The Trans. of the Institute of Electronics, Information and Communication Engineers A, Vol.J79-A, No.2, pp. 318-328, 1996.
Membership in Learned Societies:
• The Institute of Electronics, Information and Communication Engineers (IEICE)
• Information Processing Society of Japan (IPSJ)
• The Japan Society of Mechanical Engineers (JSME)
• The Institute of Electrical and Electronics Engineers (IEEE)

Name:
Yoshiyuki Tanaka

Affiliation:
Department of Artificial Complex Systems Engineering, Hiroshima University

Address:
1-4-1 Kagamiyama, Higashi-hiroshima, Hiroshima 739-8527, Japan
Brief Biographical History:
2001- Research Associate with the Faculty of Information Sciences, Hiroshima City University
2002- Research Associate in the Department of Artificial Complex Systems Engineering at Hiroshima University
Main Works:
• Y. Tanaka, T. Tsuji, V. Sanguineti, and P. G. Morasso, "Bio-mimetic Trajectory Generation using a Neural Time Base Generator," Journal of Robotic Systems, Vol.22, No.11, pp. 625-637, 2005.
Membership in Learned Societies:
• The Robotics Society of Japan (RSJ)
• Institute of Electrical Engineering of Japan (IEEJ)
• The Society of Instrumentation and Control Engineers in Japan (SICE)
• The Institute of Electrical and Electronics Engineers (IEEE)

Name:
Nan Bu

Affiliation:
Research Scientist, National Institute of Advanced Industrial Science and Technology

Address:
Shunku 807-1, Tosu, Saga 841-0052, Japan
Brief Biographical History:
2002- Doctor Course, Graduate school of Eng., Hiroshima University
2005- Postdoctoral Research Fellow, Hiroshima University
2005- National Institute of Advanced Industrial Science and Technology
Main Works:
• "MMI-based Training for a Probabilistic Neural Network," Proceedings of 2003 International Joint Conference on Neural Networks, pp. 2661-2666, USA, 2003.
• "FPGA implementation of a probabilistic neural network," The IEICE Transaction on Information and Systems, PT. 2 (Japanese Edition), Vol.J88-D-II, No.2, pp. 390-397, 2005.
Membership in Learned Societies:
• The Institute of Electrical and Electronics Engineers (IEEE)

Name:
Seishiro Sakaguchi

Affiliation:
Department of Artificial Complex Systems Engineering, Hiroshima University

Address:
1-4-1 Kagamiyama, Higashi-hiroshima, Hiroshima 739-8527, Japan
Brief Biographical History:
2000- Faculty of Engineering, Hiroshima University
2004- Graduate School of Engineering, Hiroshima University
Main Works:
• "LMI-Based Neurocontroller for Guaranteed Cost Control of Uncertain Time-Delay Systems," in Proc. of the IEEE International Symposium on Circuits and Systems, pp. 3047-3050, 2005.

Name:
Toshio Tsuji

Affiliation:
Department of Artificial Complex Systems Engineering, Hiroshima University

Address:
1-4-1 Kagamiyama, Higashi-hiroshima, Hiroshima 739-8527, Japan
Brief Biographical History:
1985- Research Associate in Faculty of Engineering at Hiroshima University
1994- Associate Professor in Faculty of Engineering at Hiroshima University
2002- Professor of Department of Artificial Complex Systems Engineering at Hiroshima University
Main Works:
• T. Tsuji, P. Morasso, K. Goto, and K. Ito, "Human Hand Impedance Characteristics during Maintained Posture in Multi-Joint Arm Movements," Biological Cybernetics, Vol.72, pp. 475-485, 1995.
Membership in Learned Societies:
• The Robotics Society of Japan (RSJ)
• The Japan Society of Mechanical Engineers (JSME)
• The Society of Instrumentation and Control Engineers in Japan (SICE)
• The Institute of Electrical and Electronics Engineers (IEEE)